PHYSICAL REVIEW D VOLUME 16, NUMBER 1 1 JULY 1977

Strange-particle cross sections from π^+p interactions at 10.3 GeV/c

M. C. Goddard, D. Gilbert, and A. W. Key*
Department of Physics, University of Toronto, Toronto, Canada M5S 1A7

H. A. Gordon and K. W. Lai†
Brookhaven National Laboratory, Upton, New York 11973
(Received 9 December 1976)

Cross sections are presented for production of final states with two strange particles from π^+p interactions at 10.3 GeV/c in a 31.1-event/μb bubble-chamber experiment.

EXPERIMENTAL DETAILS

The data described in this report were obtained from a 580 000-picture exposure of the SLAC 82-in. bubble chamber using an rf-separated π^+ beam of momentum 10.3 GeV/c with a spread of 5%. The beam flux was approximately 11 tracks per picture. The rf separator and a Čerenkov counter reduced the non-π^+ hadron part of the beam to less than 0.25%.[1] Addition of $\frac{1}{4}$ in. of lead radiator made the positron contamination negligible. Further details of the bubble chamber and the beam can be found elsewhere.[2,3]

SCANNING AND MEASURING

The film was scanned for events with a visible strange-particle decay (either V^0 or $V^{\pm}$). V^0's with zero opening angle in all views were scanned as γ's and deleted. The ionization of nonminimum tracks was recorded and stopping tracks were flagged. A beam-track count was taken every twenty frames.

To determine the number of strange-particle events missed in the scanning stage, a portion of the film was rescanned. Misidentified events (such as γ conversions, π-μ-e decays, etc.) as determined from kinematic reconstruction and visual examination were deleted from the two scans. The number of remaining events found by both scans and the number found in only one scan were used to determine the scanning efficiency.[4] This was found to vary from $52\pm5\%$ for six prongs with a V^+, to $79\pm3\%$ for four-prong events with a V^0. The errors in the efficiencies are estimates. They are an order of magnitude larger than the statistical errors.[4] Events with a V^+ only are very difficult to recognize and the efficiency for these types of events is correspondingly low. All topologies with a V^0 had scanning efficiencies greater than 70%.

The film was divided between Brookhaven and Toronto. At Toronto the measuring was done manually, on image-plane digitizers with a least count of two microns. At Brookhaven the film was measured on the Hough-Powell device.

MICROBARN EQUIVALENT

The hydrogen density was determined from a sample of π-μ-e decays to be[5]

$$\rho=(3.64\pm0.03)\times10^{22}\ \text{protons/cm}^3$$

(see Ref. 6) yielding a mean interaction length in hydrogen of

$$l_0=\frac{1}{\rho\sigma}=(1.11\pm0.02)\times10^3\ \text{cm}$$

(see Ref. 7).

We used only events with a beam interaction falling inside a fiducial volume imbedded in the bubble chamber. The distribution of beam vertices in the x (beam) direction is shown in Fig. 1. After correction for beam attenuation, this fiducial length corresponds to a mean length in the bubble chamber before interaction of 135.0 ± 0.2 cm.

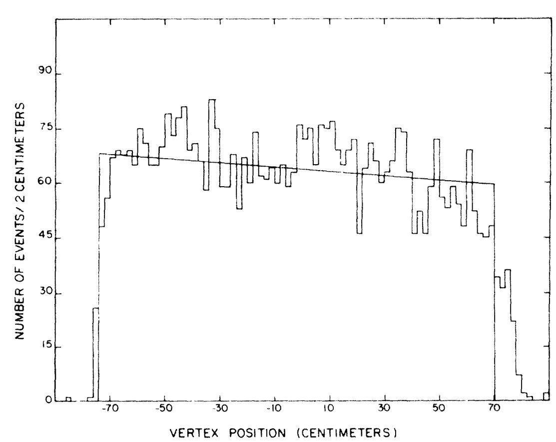

FIG. 1. Distribution of main vertices along the beam direction in the bubble chamber. The fiducial volume and the falloff expected from beam attenuation are indicated.

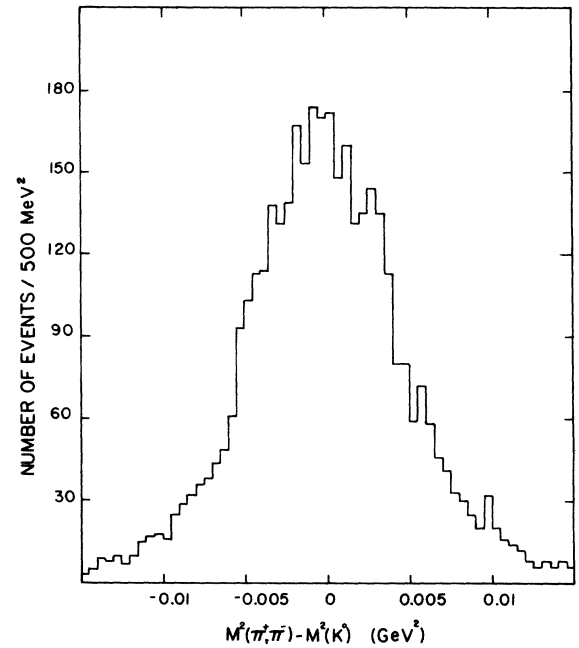

FIG. 2. $M^2(\pi^+,\pi^-) - M^2(K^0)$ from measured V^0's (mean = − 60 MeV$^2/c^4$, standard deviation = 5.4×10^3 MeV$^2/c^4$).

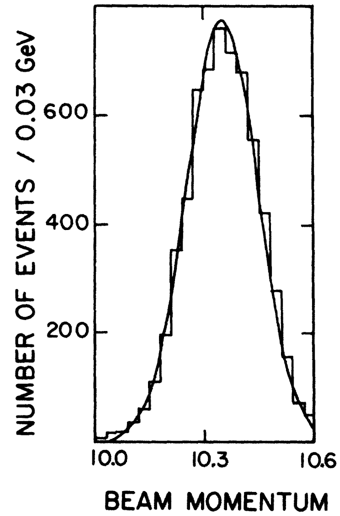

FIG. 3. Fitted beam momentum. Average is 10.35 GeV/c and full width at half maximum is 229 MeV/c.

The total path length in hydrogen is thus

$$L = (852.5 \pm 1.4)\times 10^6 \text{ cm},$$

yielding a microbarn equivalent of

$$\frac{1}{\sigma_0} = \rho L = 31.1 \pm 0.2 \text{ events}/\mu\text{b}.$$

MAGNETIC FIELD

The magnetic-field map of the chamber, as coded into the reconstruction programs,[8] was checked by calculating the K^0 mass from the measurements of the decay tracks. A decrease of the measured field by 0.5% and the removal of a small positional correlation was required to produce the distribution of the K^0 mass shown in Fig. 2.

BEAM MOMENTUM

The beam is dispersed in the horizontal direction just before entering the bubble chamber, leading to a momentum spectrum of 5 cm per percent $\Delta p/p$. We used a sample of four-constraint, nonstrange fits to parameterize the beam momentum as a function of its position on entering the chamber.[5] This gave a precise determination of the momentum for any beam track and was used as the measured input into the reconstruction programs. Figure 3 shows the distribution of the fitted beam momentum.

TABLE I. Visible decays fitted and fitted values for $c\tau$.

	Decay mode	Fraction (%)	$c\tau$ (cm) [a]	Fitted $c\tau$ (cm)
V^0	$\Lambda\to p\pi^-$	64.2	7.7	7.7 ±0.2
	$K_S^0\to\pi^+\pi^-$	68.8	2.66 [b]	2.51±0.06
	$\gamma\to e^+e^-$			
$V^\pm$	$\Sigma^+\to p\pi^0$	51.6	2.4	Not used for cross sections
	$\Sigma^+\to n\pi^+$	48.4	2.4	2.6 ± 0.2
	$\Sigma^-\to n\pi^-$	100	4.4	5.6 ± 0.8
	$K^\pm\to\pi^\pm\pi^0$	21.1		
	$K^\pm\to\mu^\pm\nu$	63.5		
	$\pi^\pm\to\mu^\pm\nu$	100		

[a] From Particle Data Group, Rev. Mod. Phys. 48, S1 (1976).
[b] This value was 2.58 in 1972.

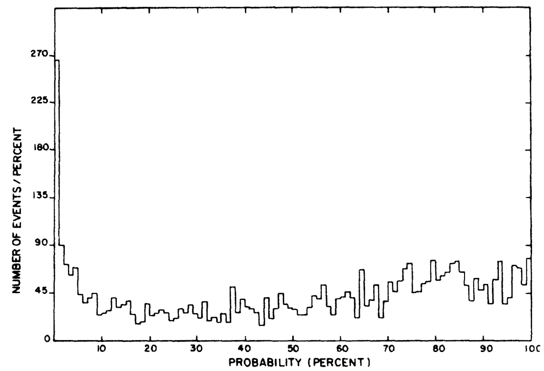

FIG. 4. χ^2 probability distribution.

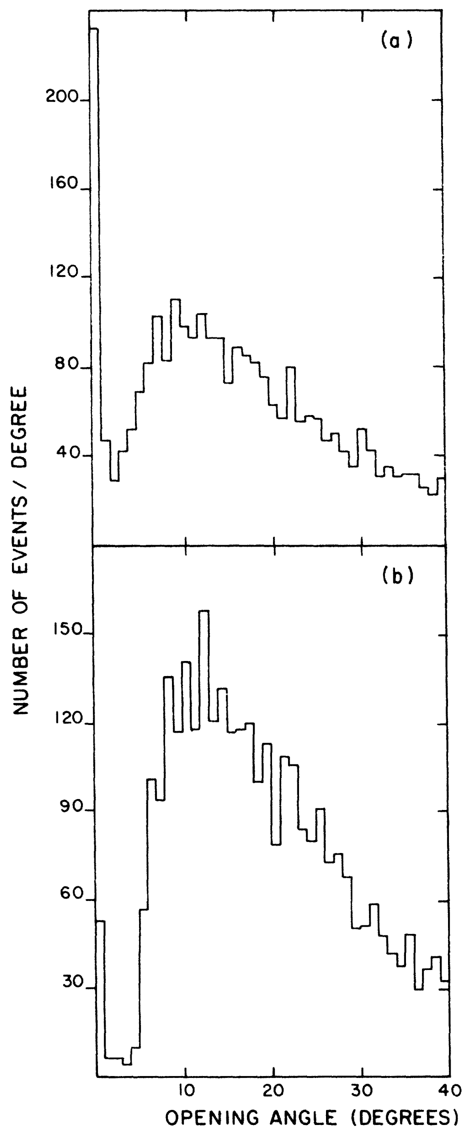

FIG. 5. (a) Space opening angle for Λ's. (b) Space opening angle for K^0's.

EVENT RECONSTRUCTION

The events were processed through the TVGP-SQUAW[9] reconstruction system. Table I shows the decay modes of the visible strange particles which we fit. We also attempt to fit a γ conversion to the V^0 and a $\pi^\pm$ decay to the $V^\pm$.

For each event the film bubble density was checked against the prediction of the fits. Inconsistent fits and events with decays fitting only nonstrange particles were deleted. Events which had apparently good visible strange particles but no fits were sent back for remeasurement. Of those fits remaining, only those in the highest constraint class were kept.[10] Fits with a χ^2 probability less than 2% were deleted (see Fig. 4) and a correction factor was applied for good events lost. The remaining fits were flagged as ambiguous.

Figure 5 shows the (space) opening angle for V^0's. The accumulation of events near zero degrees is due to γ contamination. These events were removed by deleting all visible K^0's with opening angle less than four degrees and visible Λ's with opening angle less than two degrees.

Since the scanning was done in at least two views there was a negligible[11] loss of good V^0's with a projected opening angle of zero degrees after the γ contamination was removed.

Figure 6 shows a loss of V^0 events whose film distance before decay is so small that they appear to be part of the main vertex. V^0's with a projected decay length of less than 0.5 cm were rejected and the remaining events corrected for this loss.

Figure 7 shows the projected decay length for $\Sigma^\pm$ events. Σ^+ (Σ^-) events were deleted if they had a projected decay length of less than 0.5 (1.0) cm

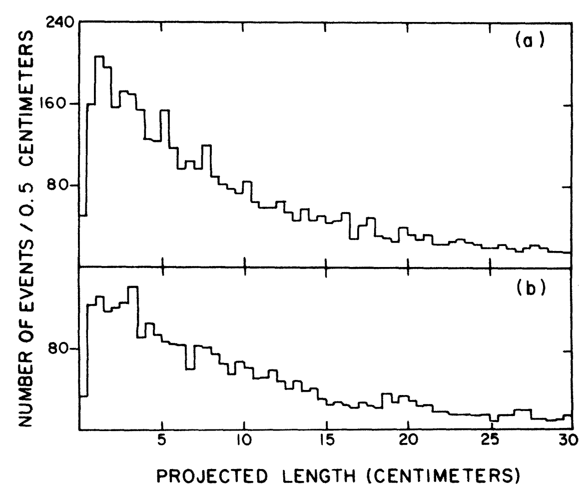

FIG. 6. (a) Projected distance between K^0 production and decay. (b) Projected distance between Λ production and decay.

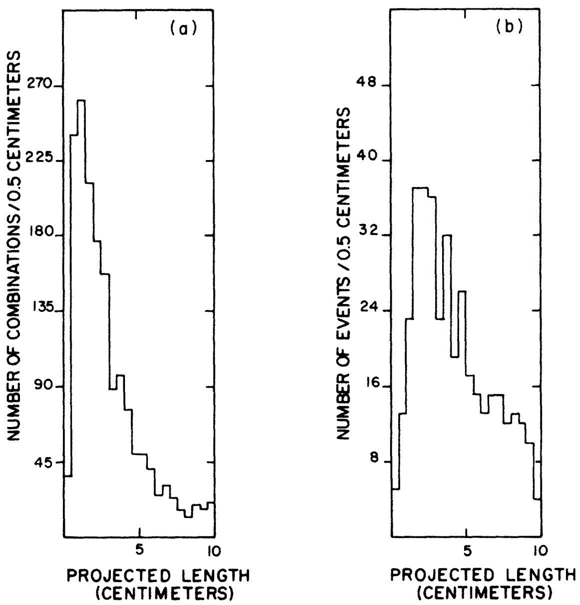

FIG. 7. (a) Projected distance between Σ^+ production and decay. (b) Projected distance between Σ^- production and decay.

or a projected opening angle of less than four (seven) degrees. A corresponding correction was applied to the remaining events.[12]

Figure 8 shows the proper lifetime ($L/\gamma\beta c$) of the visible strange particles. The falloff of events with short decay lengths is evident. The events were fitted to an exponential over the indicated ranges to give values for $c\tau$ for each particle, as listed in Table I.

WEIGHTING

Based on the four-momentum of each strange particle, each fit for every event was assigned a weight to correct for those events which failed the cuts on decay length or opening angle or had non-visible decays.[13,14] Table II shows sample averaged values for the weights of the individual strange particles. The weight for any fit was the product of the weights of the constituent strange particles.

The $K_S^0 K_S^0$ cross sections come directly from events with both K^0's visible in the bubble chamber (a K_L^0 will decay in our bubble chamber only about 0.2% of the time). The cross sections for $K_S^0 K_L^0$ channels are determined from the events with one visible K^0 after subtracting off those single-V^0 events which are $K_S^0 K_S^0$.

RESULTS

Table III lists our results for the cross sections along with the initial number of events used in each

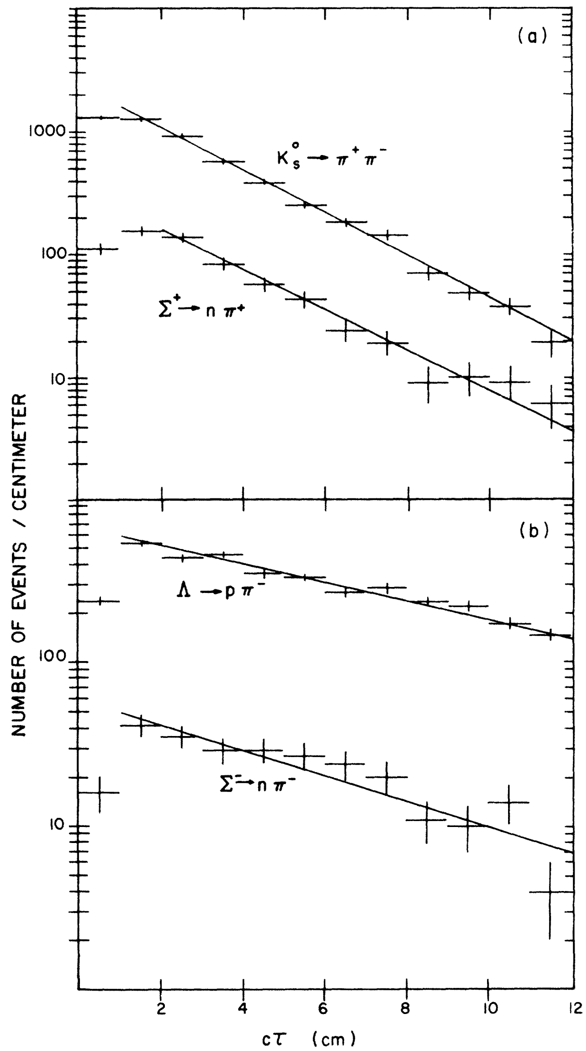

FIG. 8. (a) Proper-time distribution for $K_S^0 \to \pi^+\pi^-$ and $\Sigma^+ \to n\pi^+$. (b) Proper-time distribution for $\Lambda \to p\pi^-$ and $\Sigma^- \to n\pi^-$ (fitted lines give values for $c\tau$ given in Table I).

TABLE II. Sample-averaged weights for either visible (fitted decay) or invisible (inferred from energy-momentum conservation) strange particles.

$W(\Sigma^+)_{vis} = 3.1$	$W(K^-)_{vis} = 55$ [a]
$W(\Sigma^-)_{vis} = 1.5$	$W(K^-)_{inv} = 1.1$
$W(\Lambda)_{vis} = 1.7$	$W(K_S^0)_{vis} = 1.6$
$W(\Lambda)_{inv} = 2.5$	$W(K_S^0)_{inv} = 2.7$
$W(K^+)_{vis} = 30$ [a]	$W(K^0)_{vis} = 2W(K_S^0)_{vis} = 3.2$
$W(K^+)_{inv} = 1.1$	$W(K^0)_{inv} = \frac{2W(K_S^0)_{inv}}{W(K_S^0)_{inv}+1} = 1.5$

[a] Because of the small probability of a $K^\pm$ decaying in the bubble chamber, events with a visible $K^\pm$ were not used for cross-section determination.

TABLE III. Number of events observed and cross sections, for various channels.

Channel	No. of events	Cross section (μb)	Channel	No. of events	Cross section (μb)
$nK_S^0K_S^0\pi^+\pi^+$	63	8.5±1.5	$\Lambda K^+\pi^+$	321	30±2
$nK_S^0K_S^0\pi^+\pi^+\pi^+\pi^-$	35	5.5±1.5	$\Lambda K^+\pi^+\pi^0$	909	87±3
$nK^+\bar{K}^0\pi^+$	281	46±12	$\Lambda K^+\pi^+\pi^+\pi^-$	389	40±3
$nK^+\bar{K}^0\pi^+\pi^+\pi^-$	402	71±25	$\Lambda K^+\pi^+\pi^+\pi^-\pi^0$	1148	117±4
$nK^+\bar{K}^0\pi^+\pi^+\pi^+\pi^-\pi^-$	80	15.5±1.5	$\Lambda K^+\pi^+\pi^+\pi^+\pi^-\pi^-$	114	11.5±1.5
$nK^-K^0\pi^+\pi^+\pi^+$	86	16±4	$\Lambda K^+\pi^+\pi^+\pi^+\pi^-\pi^-\pi^0$	274	29±2
$nK^-K^0\pi^+\pi^+\pi^+\pi^+\pi^-$	21	4±1	$\Sigma^0K^0\pi^+\pi^+$	42	13±3
$pK_S^0K_S^0\pi^+$	174	23±5	$\Sigma^0K^0\pi^+\pi^+\pi^+\pi^-$	10	6±2
$pK_S^0K_L^0\pi^+$	490	40±8	$\Sigma^0K^0\pi^+\pi^+\pi^+\pi^+\pi^-\pi^-$	2	1±0.5
$pK_S^0K_S^0\pi^+\pi^0$	145	20±1.5	$\Sigma^0K^+\pi^+$	82	7.5±1.5
$pK_S^0K_S^0\pi^+\pi^+\pi^-$	84	12.5±1.5	$\Sigma^0K^+\pi^+\pi^+\pi^-$	142	14.5±1.5
$pK_S^0K_L^0\pi^+\pi^+\pi^-$	397	34±4	$\Sigma^0K^+\pi^+\pi^+\pi^+\pi^-\pi^-$	31	3±1
$pK_S^0K_S^0\pi^+\pi^+\pi^-\pi^0$	65	6±3	$\Sigma^+K^0\pi^+$	66	27±4
$pK_S^0K_S^0\pi^+\pi^+\pi^+\pi^-\pi^-$	4	1±0.5	$\Sigma^+K^0\pi^+\pi^0$	23	33±7
$pK_S^0K_L^0\pi^+\pi^+\pi^+\pi^-\pi^-$	34	5±2	$\Sigma^+K^0\pi^+\pi^+\pi^-$	87	29±3
$pK_S^0K_S^0\pi^+\pi^+\pi^+\pi^-\pi^-\pi^0$	3	1±0.5	$\Sigma^+K^0\pi^+\pi^+\pi^-\pi^0$	34	44±8
$pK^+\bar{K}^0$	179	30.5±2	$\Sigma^+K^0\pi^+\pi^+\pi^+\pi^-\pi^-$	12	3±1
$pK^+\bar{K}^0\pi^0$	551	99±5	$\Sigma^+K^0\pi^+\pi^+\pi^+\pi^-\pi^-\pi^0$	4	5±3
$pK^+\bar{K}^0\pi^+\pi^-$	395	73±4	Σ^+K^+	41	20±4
$pK^+\bar{K}^0\pi^+\pi^-\pi^0$	844	160±6	$\Sigma^+K^+\pi^0$	77	30±4
$pK^+\bar{K}^0\pi^+\pi^+\pi^-\pi^-$	119	22.5±2	$\Sigma^+K^+\pi^+\pi^-$	86	28±3
$pK^+\bar{K}^0\pi^+\pi^+\pi^-\pi^-\pi^0$	184	35±3	$\Sigma^+K^+\pi^+\pi^-\pi^0$	171	59±5
$pK^-K^0\pi^+\pi^+$	250	46±5	$\Sigma^+K^+\pi^+\pi^+\pi^-\pi^-$	19	8±2
$pK^-K^0\pi^+\pi^+\pi^0$	385	72±5	$\Sigma^+K^+\pi^+\pi^+\pi^-\pi^-\pi^0$	43	17±3
$pK^-K^0\pi^+\pi^+\pi^+\pi^-$	93	17.5±2	$\Sigma^-K^0\pi^+\pi^+\pi^+$	54	10±2
$pK^-K^0\pi^+\pi^+\pi^+\pi^-\pi^0$	122	24±2	$\Sigma^-K^0\pi^+\pi^+\pi^+\pi^0$	14	11±3
$\Lambda K^0\pi^+\pi^+$	728	43±6	$\Sigma^-K^0\pi^+\pi^+\pi^+\pi^+\pi^-$	10	2±1
$\Lambda K^0\pi^+\pi^+\pi^0$	215	62±10	$\Sigma^-K^0\pi^+\pi^+\pi^+\pi^+\pi^-\pi^0$	3	2.5±1.5
$\Lambda K^0\pi^+\pi^+\pi^+\pi^-$	690	42±9	$\Sigma^-K^+\pi^+\pi^+$	33	6±1
$\Lambda K^0\pi^+\pi^+\pi^+\pi^-\pi^0$	146	45±8	$\Sigma^-K^+\pi^+\pi^+\pi^0$	84	17±2
$\Lambda K^0\pi^+\pi^+\pi^+\pi^+\pi^-\pi^-$	123	10±4	$\Sigma^-K^+\pi^+\pi^+\pi^+\pi^-$	14	2±1
$\Lambda K^0\pi^+\pi^+\pi^+\pi^+\pi^-\pi^-\pi^0$	13	7±2	$\Sigma^-K^+\pi^+\pi^+\pi^+\pi^-\pi^0$	34	6±1

channel. The analysis of the experiment was carried out independently at Brookhaven and Toronto, thus giving two values for the cross sections for most channels. In addition, the cross sections for some channels can be calculated several ways by using events with either one or two visible decays. For instance, the cross section for $\Lambda^0K^0\pi^+\pi^+$ can be calculated using the events with one visible Λ^0, or those events with one visible K^0, or those events with both strange particles visible.[15] This gave several independent values for the cross sections. The cross-section measurements from the different topologies, from the Brookhaven and from the Toronto data, were combined to form an average cross section and error for each channel. This average value and the different cross-section measurements were used to compute a χ^2 for each channel. If this χ^2 was greater than its expectation value, the errors on the measurements were scaled up until it was equal to its expectation value (e.g., the channel $nK^+\bar{K}^0\pi^+\pi^+\pi^-$).

The cross sections were calculated both by using the "best" fit (i.e., the fit with the lowest χ^2) if the event was ambiguous and by weighting ambiguous fits by the reciprocal of the number of ambiguities. The two methods gave almost identical results, so the method of using the best fit was arbitrarily chosen.

Correcting for unfitted channels, we find the total strange-particle cross section at this energy to be 3.2 ± 0.4 mb. This is shown in Fig. 9 along with values at other energies (from Refs. 16–19).

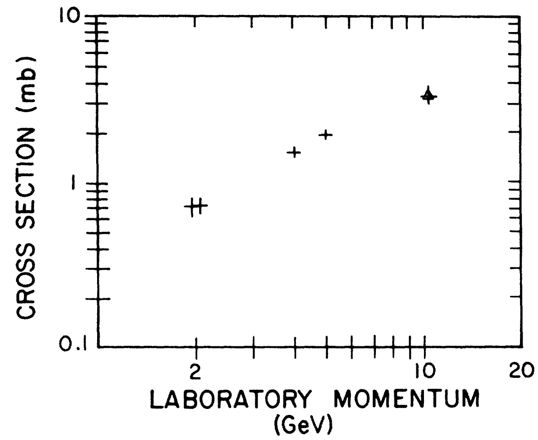

FIG. 9. Total strange-particle cross section vs laboratory momentum.

ACKNOWLEDGMENTS

This experiment could not have taken place without the participation of a large number of people. We want to especially thank those physicists who took part in the early stages of the experiment and made important contributions to its progress: Dave Crennell, George Luste, Popat Patel, Jim Prentice, Susan Vallet, and Taek-Soon Yoon. Equally important was the work of measuring, scanning, programming, and data handling. In particular, we want to thank the following who contributed so much in these areas: Quais Ashraf, Bruce Bolin, Rodney Jones, Peter Kahan, Dave Kesterton, June Liu, Sheila Maggs, Dave McDonald, John Phillips, Alfred Sipprell, and the large band of measurers and scanners at Toronto and Brookhaven. We also express our appreciation to the POLLY group and all the members of the SLAC staff who contributed to the success of the data acquisition.

*Work supported in part by the National Research Council of Canada.

†Work supported by U. S. Energy Research and Development Administration.

[1]SLAC Memo No. 8 (unpublished).

[2]SLAC Users Handbook (unpublished).

[3]S. Flatté, Lawrence Radiation Laboratory, Berkeley (LRL) Report No. LRL 646, 1968 (unpublished).

[4]S. Meyer, Rev. Sci. Instrum. 37, 662 (1966).

[5]M. Goddard, M.S. thesis, University of Toronto, 1975 (unpublished).

[6]This corresponds to a muon range of 1.072 ± 0.055 cm [P. Davis, LRL Report No. LRL 656, 1968 (unpublished)].

[7]$\sigma_T = 24.8 \pm 0.2$ mb [W. Galbraith, E. Jenkins, T. Kycia, B. Leontic, R. Phillips, A. Read, and R. Rubinstein, Phys. Rev. 138, B913 (1965)].

[8]J. Cobb, SLAC Report No. SLAC-TN-71-15, 1971 (unpublished); S. Flatté and F. Solmitz, LRL Report No. LRL 663, 1968 (unpublished).

[9]F. Solmitz, A. Johnson, and T. Day, LRL Programmer's Note No. P-117, 1965 (unpublished); O. Dahl, T. Day, F. Solmitz, and N. Gould, LRL Programmer's Note No. P-126, 1968 (unpublished).

[10]Studies using artificially generated events show that it is unlikely that events with missing neutrals can be fitted as fully constrained events. For the case of the (Σ^0- Λ) ambiguity see W. Butler, D. Coyne, G. Goldhaber, J. MacNaughton, and G. Trilling, Phys. Rev. D 7, 3177 (1973).

[11]We estimate less than 1% for Λ and less than 2% for K^0 (see Ref. 5).

[12]Since the $\Sigma^+ \rightarrow p\pi^0$ decay has such a small opening angle, only events with $\Sigma^+ \rightarrow n\pi^+$ were used for cross-section determination.

[13]M. Goddard, Ph.D. thesis, University of Toronto, 1977 (unpublished).

[14]R. Hemingway and H. Whiteside, University of Maryland Technical Report No. 70-065, 1969 (unpublished).

[15]In these cases the number of events, as listed in Table III, is the sum of the events in the different topologies contributing to the channel. This explains why some channels have an apparently large number of events but a small cross section.

[16]D. Toet, C. Pols, D. Schotanus, R. Van de Walle, P. Thuan, B. Wessels, G. Winter, J. Major, G. Rinaudo, and A. Werbrouck, Nucl. Phys. B63, 248 (1973).

[17]J. Bartsch, L. Bondar, R. Speth, G. Hotop, G. Knies, F. Storim, J. Brownlee, N. Biswas, D. Lueers, N. Schmitz, R. Seelinger, and G. Wolf, Nuovo Cimento 43A, 1010 (1966).

[18]F. James and H. Kraybill, Phys. Rev. 142, 896 (1966).

[19]S. Dagan, Z. Ma, J. Chapman, L. Fortney, and E. Fowler, Phys. Rev. 161, 1384 (1967).